Journal of Software Engineering

ISSN 1819-4311

Academic Journals Inc.

www.academicjournals.com

Journal of Software Engineering 8 (4): 345-360, 2014
ISSN 1819-4311 / DOI: 10.3923/jse.2014.345.360

Simulation and Experiment of 50% Calcium Oxide-sand Mixture in a Bubbling Fluidized Bed CO_2 Absorption Reactor

[1]M.M. Mahadzir, [1]A.R. Hemdi, [2]Z.A. Zainal, [3]N.I. Ismail and [3]M. Hisyam Basri
[1]Faculty of Mechanical Engineering, Universiti Teknologi MARA (UiTM), Pulau Pinang, Malaysia
[2]School of Mechanical Engineering, Universiti Sains Malaysia (USM), Engineering Campus, Pulau Pinang, Malaysia
[3]Automotive Research and Testing Centre (ARTeC), Universiti Teknologi MARA (UiTM), Pulau Pinang, Malaysia

Corresponding Author: M.M. Mahadzir, Faculty of Mechanical Engineering, Universiti Teknologi MARA (UiTM), Pulau Pinang, Malaysia

ABSTRACT

The overwhelming increasing the fuel price and exhausting of fossil fuel resources in Malaysia is alarming, therefore, renewal sources of energy should be further studied. There are attempts in using biomass as renewable energy resources to produce producer gas which can be used as fuel, however, the shortcomings and inefficiencies in the available technology have made it uneconomical. The CO_2 in the producer gas which is incombustible from the biomass gasification must be removed to enhance its quality. For that, a device called Bubbling Fluidized Bed CO_2 Absorption Reactor (CO_2 BFBAR) has to be developed. Calcium oxide (CaO) derived from natural limestone produced in Malaysia (blessed with abundant reserve of limestone resources) can be an effective sorbent to absorb carbon dioxide (CO_2) gas at high temperature. In the present study, the simulation of the hydrodynamic characteristics in the CO_2 BFBAR is done. The objective is to find out whether the 50% CaO-sand mixture used in the reactor can perform fluidization perfectly without sticking out. The three dimensional geometry and mesh generation of the CO_2 BFBAR was build using ANSYS FLUENT CFD software and then the geometry is exported to the Computational Fluid Dynamics (CFD) software called Fluent v6.2.16 for analysis. By applying the constant volume flow rate, Q from 15 to 55 L min^{-1}, the Fluent simulated the bubbling height of CaO-sand material and the bubbling behavior in the CO_2 bfbar versus time for three types CaO particle sizes (100, 500 and 1000 μm). After that, the results from the computer simulation analysis are compared to the cold model experiment results. Overall, it shows that the simulation results give a good agreement with the experiment results. The percentages difference obtained for three types CaO particle sizes, are below than 5.3%. All results obtained have been used to design the CO_2 BFBAR.

Key words: Simulation, CaO, bubbling fluidized bed absorption reactor, CO_2 absorption

INTRODUCTION

Fuel is undoubtedly the most important source of energy in Malaysia. It has been used predominantly in power plants and to generate work in internal combustion engines. However, the extensive exploitation of fossil fuels for power has given rise to a number of serious problems namely; depletion of fuel reserves, price inflation of raw materials, adverse effects on the environment due to emissions from combustion devices and threatening level of greenhouse gas emissions.

Renewable energy offers opportunity to lower fossil fuel consumption. The use of renewable energy also provides environmental, economic and political benefits and they are also not subjected to depletion in time. One of the fuels for renewable energy is biomass. With biomass, gasification technology using a downdraft biomass gasifier, biomass raw material produced a type of gas called producer gas composed primarily of hydrogen and carbon monoxide (Klass, 1998) for internal combustion engines or coupled to turbines to generate power. According to (Rezaiyan and Cheremisinoff, 2005; McKendry, 2002), the producer gas has produced low Heating Value (HV) only around 4-6 MJ Nm^{-3} when used air as agent for gasifying.

Producer gas has small hydrogen concentration, approximately 6-20% by volume when using a downdraft biomass gasifier (Munoz *et al*., 2000; Sridhar *et al*., 2001; Zainal *et al*., 2002; Dogru *et al*., 2002; Midilli *et al*., 2002; Nam *et al*., 2004). In order to increase the percentage of the hydrogen, a new method has to be studied and developed. For instance, the producer gas from biomass gasification system contains high amount of CO_2, 15-20% (Sridhar *et al*., 2001; Dogru *et al*., 2002) thereby lower its heating value as CO_2 acts as a diluent. Removing CO_2 from the producer gas will improve its heating value and inadvertently improve the amount of combustible gases such as hydrogen, carbon monoxide and methane. The only one of the most promising method is based on the reversible absorption of CO_2 on specific metal oxides at high temperature. Carbon dioxide capture using sorbents called Calcium Oxide (CaO) has been reported by Manovic *et al*. (2009). It is because of their wide availability, low in cost, higher absorption capacity and high selectivity for CO_2. In Malaysia, CaO is blessed with abundant reserve of resources in form of limestone. Extensive limestone resources are located in the states of Perak, Pahang, Kelantan, Kedah and Negeri Sembilan. It was estimated over 10 billion tonnes of limestone resources throughout the country (Ibrahim, 2007).

To improve the producer gas HV, firstly the device called the Bubbling Fluidized Bed CO_2 Absorption Reactor (CO_2 BFBAR) to absorb CO_2 has to be developed. To do so, the 3-D Computational Fluid Dynamics (CFD) software such as Fluent 6.2.16 has to be studied and give a simulate results to know the hydrodynamic characteristics such as bubbling height of CaO material and the bubbling behavior in the CO_2 BFBAR. The CFD used a numerical approach to solve the differential equations governing transport of mass, momentum and energy in the situation of moving fluids (Anderson, 1995). The CFD studies for bubbling fluidized bed reactors have been intensively done for lab-scale or pilot-scale plants in the industries (Singh *et al*., 2013; Gomez-Barea and Leckner, 2010; Park *et al*., 2008; Zheng, 2008; Van de Velden *et al*., 2008; Cooper and Coronella, 2005). However, there are only a few numerical studies which focus on CaO as bed material in the bubbling fluidized bed reactor published by Azadi (2011), Vuthaluru *et al*. (2009) and Behjat *et al*. (2008). Therefore, it's still room for author to study the CFD modeling and focusing to CaO particularly in improving the quality of producer gas as mention in early.

In the present study, the modeling, simulation and experiment of the hydrodynamic characteristics such as the height of the bed expansion, the bubble and bed material volume fraction verses time in the CO_2 BFBAR were able to be ascertained. The objective is to find out whether the 50% CaO-sand mixture used in the reactor can perform fluidization perfectly without sticking out. Common mathematics equations used for the modeling and simulation were presented. In addition, the cold model experiment was also conducted to ensure that all data results obtained from the simulation can be validated.

METHODOLOGY

Modeling: A 3-D model of the CO_2 BFBAR is generated in ANSYS FLUENT CFD software and then the geometry is exported to the computational fluid dynamics software name Fluent v6.2.16

for analysis. The size of the 3-D model is similar to the actual size of CO_2 BFBAR. A multiphase flow consisting of gas-solid phase flow was used inside the CO_2 BFBAR model. The Euler-Euler approach in which the different phases are treated mathematically as interpenetrating continua has been chosen because this model needs less computational resources. In Fluent, Eulerian multiphase model was used to generate the multiphase flow. It is because this model allows multiple, separate and interacting phases. It solves a set of momentum and continuity equations for each phase as stated in FLUENT (2009).

Momentun equation:

For gas phase:

$$\left(\frac{\partial}{\partial t}\left(\varepsilon_g\rho_g\vec{V}_g\right)+\nabla\left(\varepsilon_g\rho_g\vec{V}_g\vec{V}_g\right)=\nabla\bar{\bar{\tau}}_g-\varepsilon_g\nabla P+\varepsilon_g\rho_g g+K_{sg}\left(\vec{V}_s-\vec{V}_g\right)\right) \tag{1}$$

where, P is the pressure, g is the gravity and K_{sg} is the drag coefficient between the gas and the solid phase. The gas phase stress tensor $\bar{\bar{\tau}}_g$ is given by:

$$\bar{\bar{\tau}}_g=\varepsilon_g\mu_g\left(\nabla\vec{V}_g+\left(\nabla\vec{V}_g\right)^T\right)+\varepsilon_g\left(\lambda_g+\frac{2}{3}\mu_g\right)\nabla\vec{V}_g\bar{\bar{I}} \tag{2}$$

For solid phase:

$$\left(\frac{\partial}{\partial t}\left(\varepsilon_s\rho_s\vec{V}_s\right)+\nabla\left(\varepsilon_s\rho_s\vec{V}_s\vec{V}_s\right)=\nabla\bar{\bar{\tau}}_s-\nabla P_s-\varepsilon_s\nabla P+\varepsilon_s\rho_s g+K_{sg}\left(\vec{V}_s-\vec{V}_g\right)\right) \tag{3}$$

where, P_s is the granular pressure, $\bar{\bar{\tau}}_s$ is the solid stress tensor and can be written as:

$$\bar{\bar{\tau}}_s=\varepsilon_s\mu_s\left(\nabla\vec{V}_s+\left(\nabla\vec{V}_s\right)^T\right)+\varepsilon_s\left(\lambda_s+\frac{2}{3}\mu_s\right)\nabla\vec{V}_s\bar{\bar{I}} \tag{4}$$

where, λ_s is the granular bulk viscosity and μ_s is the granular shear viscosity.

Continuity equation:

For gas phase:

$$\frac{\partial}{\partial t}\left(\varepsilon_g\rho_g\right)+\nabla\left(\varepsilon_g\rho_g\vec{V}_g\right)=0 \tag{5}$$

For solid phase:

$$\frac{\partial}{\partial t}\left(\varepsilon_s\rho_s\right)+\nabla\left(\varepsilon_s\rho_s\vec{V}_s\right)=0 \tag{6}$$

where, ε, ρ and $\vec{V}$ are volume fraction, density and velocity.

Grid generation: Figure 1 shows the 3-D mesh of CO_2 BFBAR domain based on the transparent perspex CO_2 BFBAR rig as shown in Fig. 2. An unstructured volume mesh of tetrahedral cells is

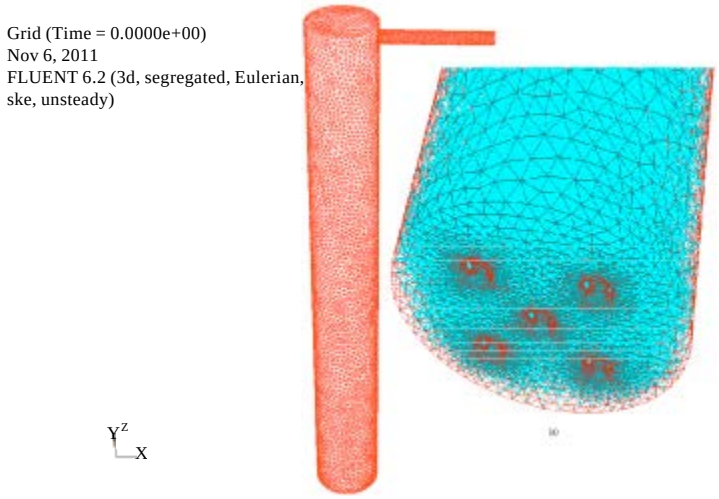

Fig. 1: Carbondioxide BFBAR 3-D meshing model with velocity inlet (boundary)

Fig. 2: Carbondioxide BFBAR rig

utilized to generate grid to the domain with the total number of 453,701. The selection of cells number has been chosen based on the grid independence analysis. Early, three distinctive grid intervals of 6, 4 and 2 mm has been meshed to the 3-D geometry of CO_2 BFBAR to simulate the hydrodynamic behavior of the bed. The 6 mm grid interval size has been chosen for the simulation to obtain reasonable time efficiency (45 h) without losing the accuracy of results. Table 1 shows all the results of the grid independence analysis obtained at superficial gas velocity of 0.214 m sec^{-1} (55 L min^{-1}), 100 micron particle size, 50% CaO-sand mixture and 2 bar pressurize air. The unstructured mesh is used for this study due to the model's complexity. Advantages of unstructured mesh are due to the decreased time required to generate grid over complicated geometries and it offer the potential to adapt the grid to improve the accuracy of the computation without incurring the penalties associated with global refinement (Anderson, 1995). Therefore, the unstructured mesh becomes a favorable type of grid.

Table 1: Grid independence analysis results

Mesh spacing (mm)	No. of cells	Pressure drop (kPa)	Simulation time for 20 sec real time (h)
6	453,701	1.35	45
4	816,618	1.41	121
2	1,034,252	1.39	215

Steps for using Eulerian multiphase model: In this section, procedures for setting up the Eulerian multiphase model and solving the multiphase problem using Fluent 6.2.16 is described in detail. The first step is to enable the Eulerian multiphase model in the multiphase model dialog box. The input for this model is the number of phases which is two (gas and particle) in this problem. Once the Eulerian multiphase model is appropriate for the study, the material representing each phase from the materials database is defined. It should be noted that since the model includes a particulate (granular) phase, hence a new material for it in the fluid materials category is created. The flow has been considered in laminar regime and since the body forces are present, gravitational acceleration (9.81 $msec^{-2}$) in the operating condition dialog box is specified.

- **Defining the phases:** In this section, defining the primary, secondary phases and their interaction (drag forces) are stated. The primary phase in this problem is the gas phase and the particles (granular materials) are the secondary phase. Primary phase is air having density of 1.16 kg m^{-3}, a specific heat of 0.994 kJ kg^{-1} K^{-1} and a viscosity of 1.7894×10^{-5} kg $msec^{-1}$. The air distribution plate was modeled as a uniform surface velocity inlet. The secondary phase which is CaO and sand were defined. For defining the material properties for the granular phase the, density is specified (example 2276 kg m^{-3}). After enabling the granular option in the secondary phase dialog box, the granular temperature model is specified and to be solved as a partial differential equation. Other properties need to be specified in the secondary phase dialog box are as following; (1) Diameter; specifies the diameter of particles which is selected constant for this problem, examples 100, 500 and 1000 μm, (2) Granular viscosity; specifies the kinetic part of the granular viscosity of the particles. In this problem, the Syamlal *et al.* (1993) model has been selected, (3) Granular bulk viscosity; specifies the solids bulk viscosity. The Lun *et al.* (1984) model has been selected, (4) Granular conductivity, specifies the solids granular conductivity. The Syamlal *et al.* (1993) model has been selected for this problem and (5) Packing limit; specifies the maximum volume fraction for the granular phase. The packing limit is about 0.63 (monodispersed spheres), which is the default value in Fluent

For granular flows, the drag function is specified to be used in the calculation of the momentum exchange coefficients and also need to specify the restitution coefficient for particle collisions. After enabling the phase interaction dialog box, the Gidaspow model has been selected as the drag function to be used in the calculation and the restitution coefficient of 0.9, which is the default value in Fluent.

- **Boundary conditions:** In this section, the procedure for setting the boundary conditions have been done. Three types of boundary conditions are used in the present study: Velocity inlet, pressure outlet and wall as shown previously in Fig. 1. For air as the primary phase, the velocity inlet boundary has been selected which is the bottom face of the CO_2 BFBAR at the nozzle distribution plate. Air enters at constant volume flow rate, Q from 15-55 L min^{-1} (2.5×10^{-4} m^{-3} sec^{-1} to 9.2×10^{-4} m^{-3} sec^{-1}). Therefore, the velocity magnitudes

are from 0.058-0.214 $msec^{-1}$. For the secondary phase which is particles, the volume fraction and velocity magnitude were set to zero for the inlet boundary.

For a pressure outlet boundary which is the top outlet of the CO_2 BFBAR, there are no conditions to be specified for the primary phase since, the flow is laminar. For the mixture phase, the backflow volume fraction was set as a constant as default value in fluent. The pressure outlet boundary condition was used by fixing the value of static pressure to 1.013×10^5 Pa. For the entire wall zone, the velocity components are set as zero considering the no-slip conditions.

- **Initialization:** Before starting CFD simulation, an initial "guess" for the solution flow field must be provided to Fluent. The value for all initial velocity components of both phases and also the pressure field was set as zero. The initial distribution of the phases was defined by patching an initial volume fraction (0.6) for the granular phase. The region to patch the volume fraction (fixed bed height) is defined as a separate cell zone. This distribution will serve as the initial condition at t = 0, for a transient simulation
- **Stability and convergence:** It is well known that the process of solving a multiphase system is inherently difficult and may encounter some stability or convergence problems. If the CPU time is a concern for transient problems, then the best option is to use Phase Coupled Semi Implicit Method for Pressure Linked Equations (PC-SIMPLE) (FLUENT, 2009). Besides that, if the solution requires higher order numerical schemes, it is recommended to start with a small time step which can be increased after performing a few time steps to get a better approximation of the pressure field. In the process of doing these, if difficulties are encountered due to higher order schemes or due to the complexities of the problem, the Courant number needs to be reduced. According to FLUENT (2009), the default Courant number in Fluent is 200 but it can be reduced to as low as 4. This can later be increased if the iteration process runs smoothly

In addition, there are explicit under-relaxation factors for velocities and pressure. All other under-relaxation factors are implicit. Lower under-relaxation factors for the volume of fraction equation may delay the solution dramatically with the coupled solver (any value 0.5 or above is adequate), otherwise PC-SIMPLE would normally need a low under-relaxation for the volume fraction equation. These are some parameters that need to be handled to improve stability and convergence behaviour of the simulation.

- **Post-processing:** Once the simulation has ended, results can be accessed through post-processing in fluent. Contours of the volume fraction of the bed material were monitored with respect to time to check the bed motion. The bed expansion height was also monitored for three different particle sizes; 100, 500 and 1000 μm at various volume flow rates. The measurements are made by measuring the height of bed material at the end of each simulated image. The scale used is in meters. Figure 3 shows the flow process of the simulation

Computational model parameters: Fluent 6.2.16 is operated on an AMD Phenom II, 2.8 GHz processor (32-bit operating system) with 4 GB RAM to solve the governing equations. The example of computational model parameters for 100 μm, 50% CaO-sand mixture is listed in Table 2.

Cold model experiment: A cold model experiment was conducted to study the hydrodynamic behavior of CO_2 BFBAR with pressurized air at ambient temperature. Figure 4 shows the

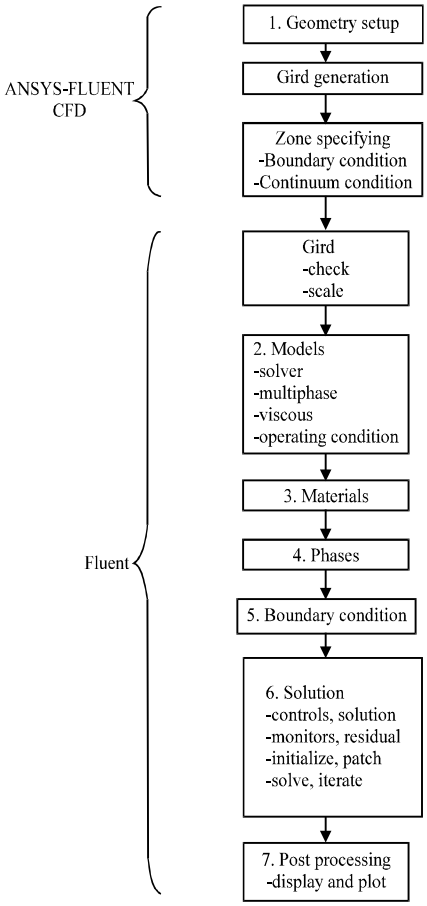

Fig. 3: Flow process of the simulation

Table 2: Computational model parameters (100 μm, 50% CaO-sand mixture)

Parameter	Values
Particals density	2276 kg m^{-3}
Air density	1.145 kg m^{-3}
Particle diameter	100 μm
Initial solid packing	0.6
Superficial velocity	0.058 m sec^{-1} (15 L min^{-1})
	0.097 m sec^{-1} (25 L min^{-1})
	0.136 m sec^{-1} (35 L min^{-1})
	0.174 m sec^{-1} (45 L min^{-1})
	0.214 m sec^{-1} (55 L min^{-1})
Bed dimention	0.6 (H)×0.074 (ID) m
Static bed height	0.075 m
Cross sectional area	4.3×10^{-3} m^2
Inlet boundary condition type	Velocity
Outlet boundry condition type	Pressure

apparatus for the cold model experiment. The CO_2 BFBAR was made of transparent perspex with an inner diameter of 74 and 600 mm height. The nozzle distributor plate has five nozzles each having four holes of 2.7 mm diameter. Detail of the CO_2 BFBAR is shown in Fig. 5.

Fig. 4: Photograph of Cold model experiment apparatus

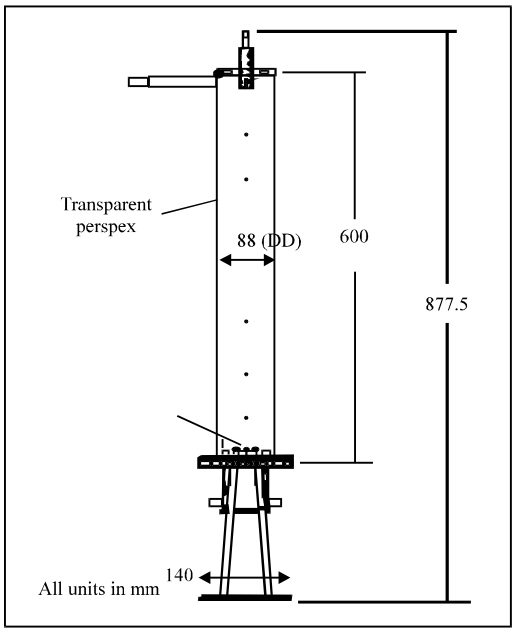

Fig. 5: Diagram of CO_2 BFBAR

CaO mixed with sand was used as the bed material in the CO_2 BFBAR. Variables affecting the fluidization height were studied such as 50% CaO-sand mixture percentages, air volume flow rates (15, 25, 35, 45, 55 L min^{-1}), 2 bar air intake pressure and different CaO particles sizes (100, 500 and 1000 μm). The detail characteristic of fluidization behavior for 1000 μm CaO has been done and published by Mahadzir *et al.* (2010).

Air flow from the air compressor was set to desired the pressures and volume flow rates. During the experiment, the hydrodynamic behaviors such as the bed expansion height and the pressure drop across the CO_2 BFBAR were recorded. Fine particles found in the filter bag was weighed and recorded at the end of each experiment. All the data recorded were analyzed.

RESULTS AND DISCUSSION

Simulation analysis: Figure 6 shows the contour of volume fraction for 50% CaO-sand mixture ratio for 100 μm particle size with 2 bar pressurized air passed through the bed on 20 sec real-time simulations. The static bed height for the material was 0.075 m. It can be observed that fluidizations occur at all volume flow rates even at 15 L min^{-1} (0.00025 m^3 sec^{-1} or 0.058 m sec^{-1}). This is because of the minimum fluidization velocity, u_{mf} is 0.0071 m sec^{-1} based on the calculation obtained using the modified Ergun equation (Yang, 2003):

$$\mu_{mf} = \frac{\mu_g}{\rho_g d_s}\left[(33.7^2 + 0.0408Ar_{numb})^{\frac{1}{2}} - 33.7\right] \quad (7)$$

Where:

μ_g : Dynamic viscosity of the carrier gas (kg $msec^{-1}$)
ρ_g : Density of the carrier gas (kg m^{-3})
d_s : Solid particles size (m)
Ar_{numb} : Archimedes number numb

Bubbles and different volume fraction in the CO_2 BFBAR were observed with increasing volume flow rates. The bubble is represented by green colored portion surrounded by yellow and red. The cloud which is a mixture of solid and gas phase is represented by yellow colored portion; this is where gas circulates in a close loop between the bubble and its surroundings. Similar trends of fluidization can also be identified in particle sizes of 500 and 1000 μm CaO with 50% CaO-sand mixture ratio. These contour volume fraction fluidization regimes are shown in Fig. 7 and 8.

Based on these observations (Fig. 6, 7 and 8), a graph of the bed height simulated by fluent versus volume flow rate for three particle sizes is plotted. Table 3 shows the data obtained. As indicated in Fig. 9, it was found that the use of large particle size of the solid material will cause the inter-particle forces or the cohesive forces to be weaker and this will allow more bubbles to be formed. Thus, generated good fluidization respect to the bed height. On the other hand, the use of fine and small particles will generate high inter-particle forces and result in low fluidization at low volume flow rate, then beginning to fluidize well and finally reaching high bed height fluidization at 55 L min^{-1}. Despite all those reactions, the fluidization between air and CaO-sand mixture has occurred using these three particles size at all volume flow rate.

Comparison between cold model experiment and simulation: The results for the cold model experiment are shown in Table 4. The bed expansion height (bed height minus static bed height) is used as a reference for the comparison. Figure 10 shows three graphs describe the comparison between fluent simulation and experiment refers to the bed expansion height. It is discovered that the bed expansion height obtained from the experiment of three particle sizes is similar to the fluent simulation modeled. The percentages of difference for three types of particle sizes used are calculated based on:

$$\left|\frac{\text{First value-second value}}{(\text{First value+second value})/2}\right| \times 100\% \quad (8)$$

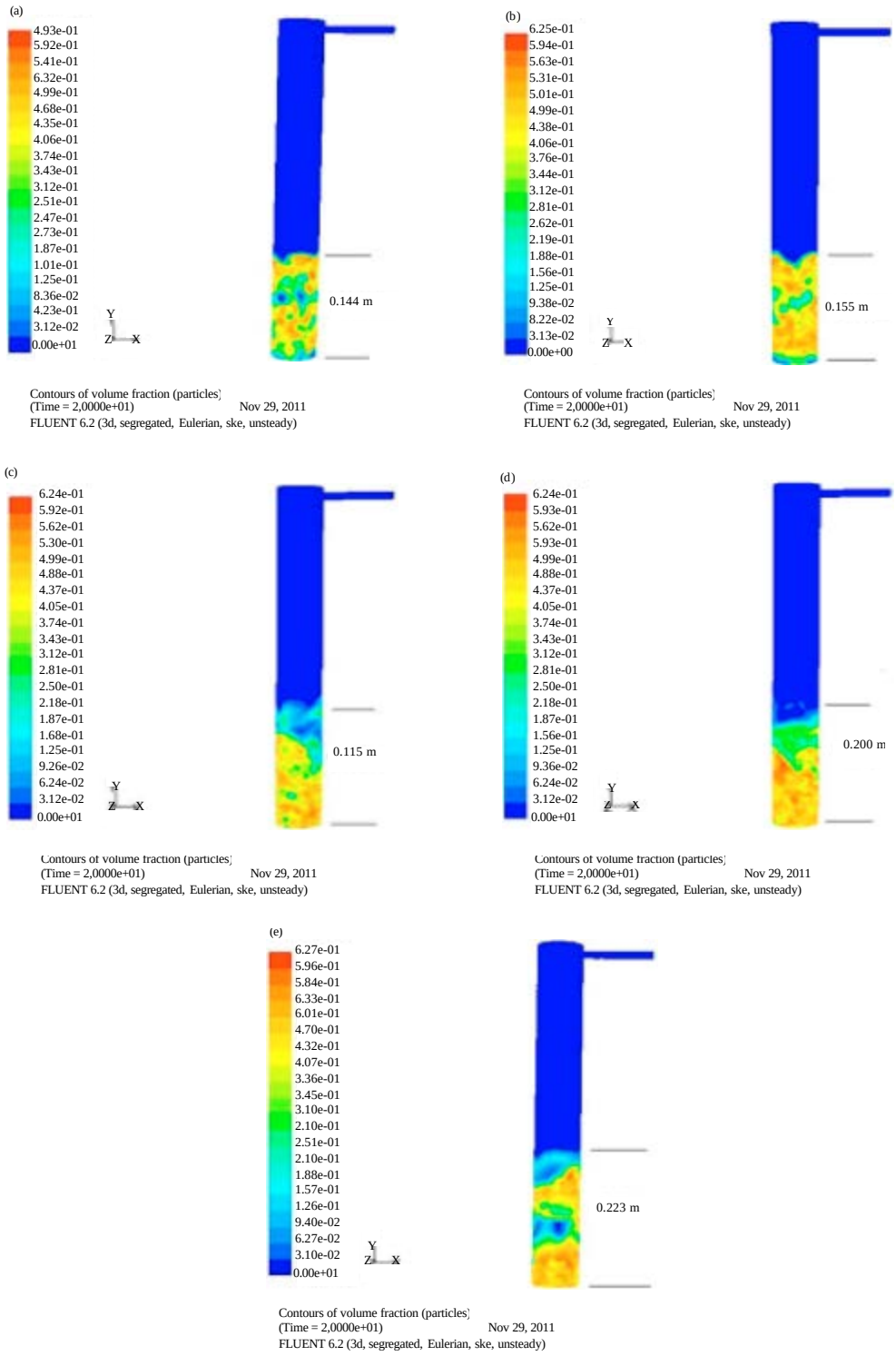

Fig. 6(a-e): Contour of volume fraction of 100 μm, 50% mixture, (a) 15 L min^{-1}, (b) 25 L min^{-1}, (c) 35 L min^{-1}, (d) 45 L min^{-1} and (e) 55 L min^{-1}

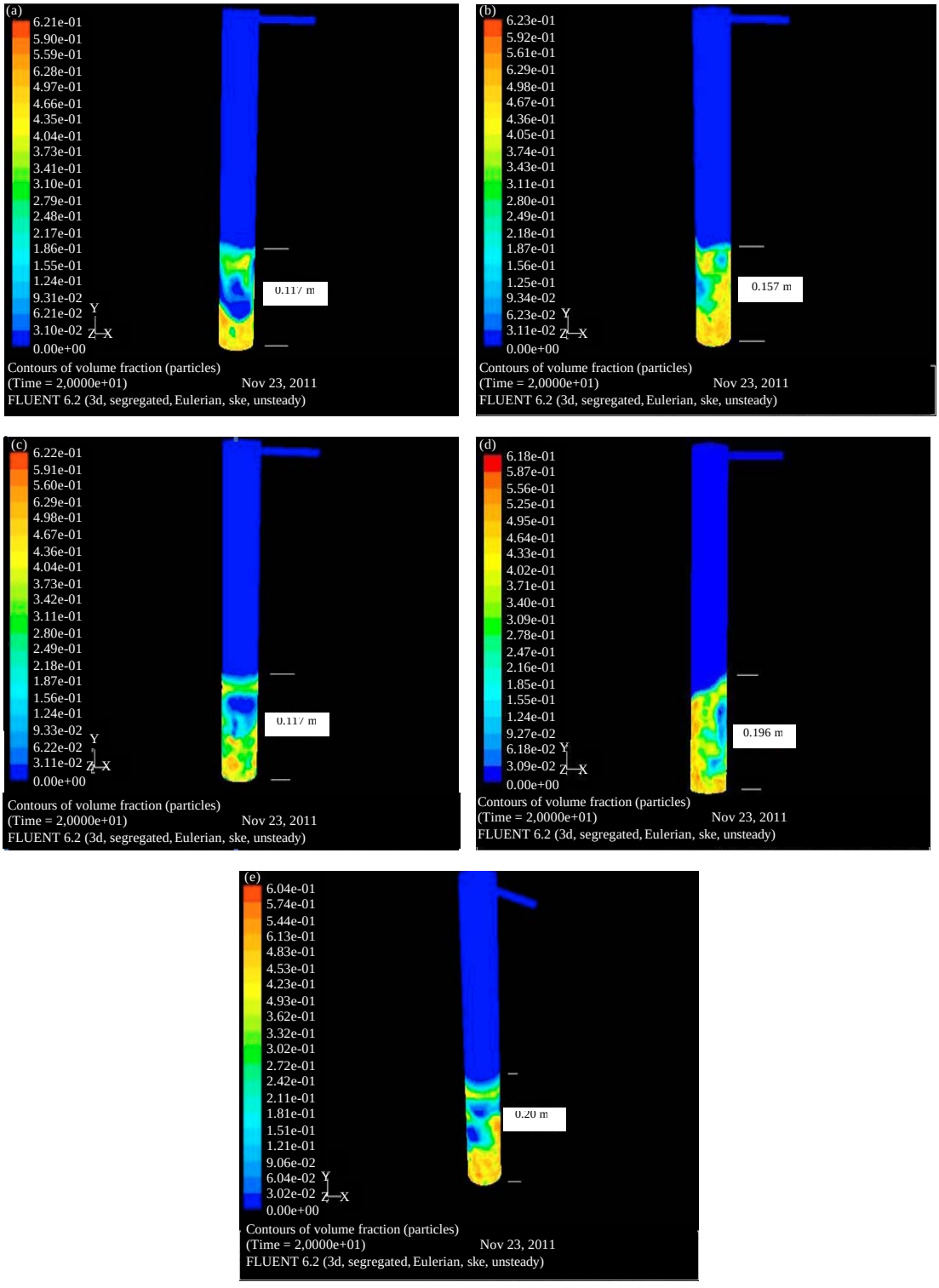

Fig. 7(a-e): Contour of volume fraction of 500 μm, 50% mixture, (a) 15 L min^{-1}, (b) 25 L min^{-1}, (c) 35 L min^{-1}, (d) 45 L min^{-1} and (e) 55 L min^{-1}

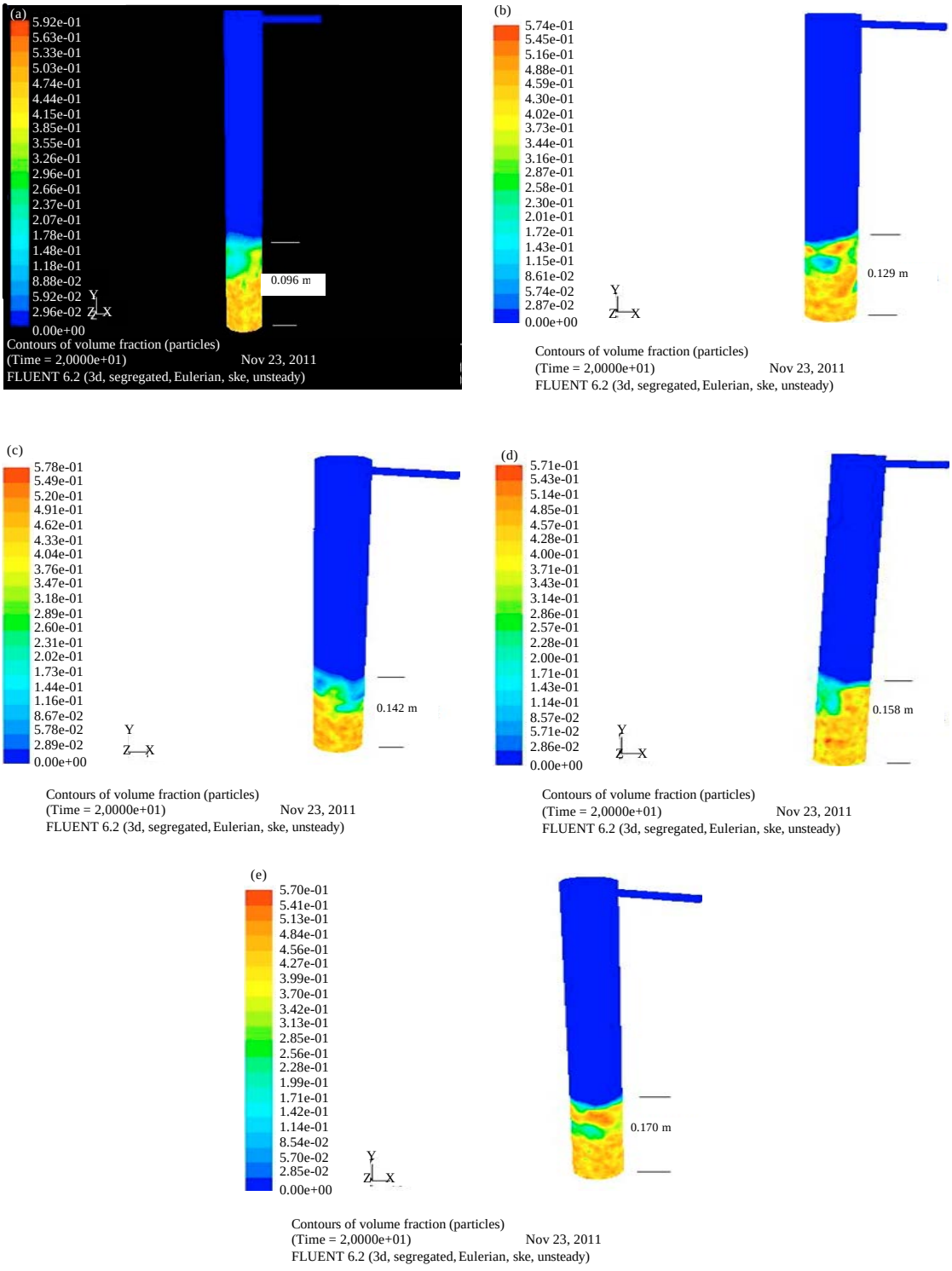

Fig. 8(a-e): Contour of volume fraction of 1000 μm, 50% mixture, (a) 15 L min^{-1}, (b) 25 L min^{-1}, (c) 35 L min^{-1}, (d) 45 L min^{-1} and (e) 55 L min^{-1}

Table 3: Results analysis from Fluent simulation

	50% mix, 2 bar (μm)		
Flow rate, Q (L min^{-1})	100	500	1000
Bed height (m)			
0	0.075	0.075	0.075
15	0.144	0.177	0.096
25	0.166	0.157	0.129
35	0.189	0.177	0.142
45	0.210	0.196	0.158
55	0.223	0.200	0.170
Bed expansion height (m)			
0	0.000	0.000	0.000
15	0.069	0.042	0.021
25	0.091	0.082	0.054
35	0.114	0.102	0.067
45	0.135	0.121	0.083
55	0.148	0.125	0.095

Table 4: Results of cold model experiment

Volume flow rate, Q (L min^{-1})	15	25	35	45	55
CaO size (100 μm), pressure (bar) 2					
Bed expansion height, Δ height (m)	0.073	0.099	0.118	0.140	0.150
CaO weight (g)	0.546	0.6	0.794	0.811	1.125
Fluidization occur	Yes	Yes	Yes	Yes	Yes
CaO size (500 μm), pressure (bar) 2					
Bed expansion height, Δ height (m)	0.045	0.085	0.1081	0.125	0.130
CaO weight (g)	0.546	0.6	0.794	0.811	1.125
Fluidization occur	Yes	Yes	Yes	Yes	Yes
CaO size (1000 μm), pressure (bar) 2					
Bed expansion height, Δ height (m)	0.020	0.050	0.070	0.080	0.090
CaO weight (g)	0.546	0.6	0.794	0.811	1.125
Fluidization occur	Yes	Yes	Yes	Yes	Yes

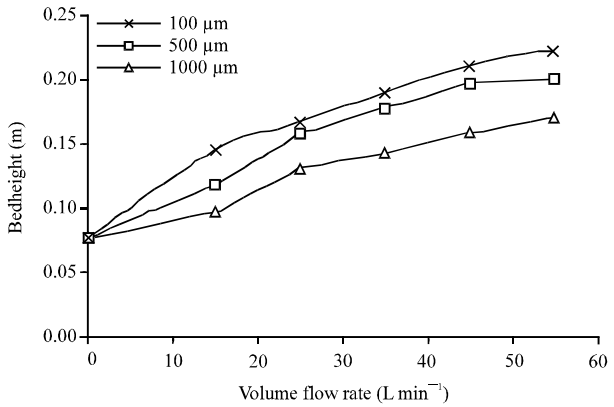

Fig. 9: Comparison between three particle sizes from Fluent simulation

The percentages of difference obtained are 4.50, 4.68 and 5.21% as shown in Table 5. The data collected therefore has supported that the developed simulation model has provided acceptable and reliable results.

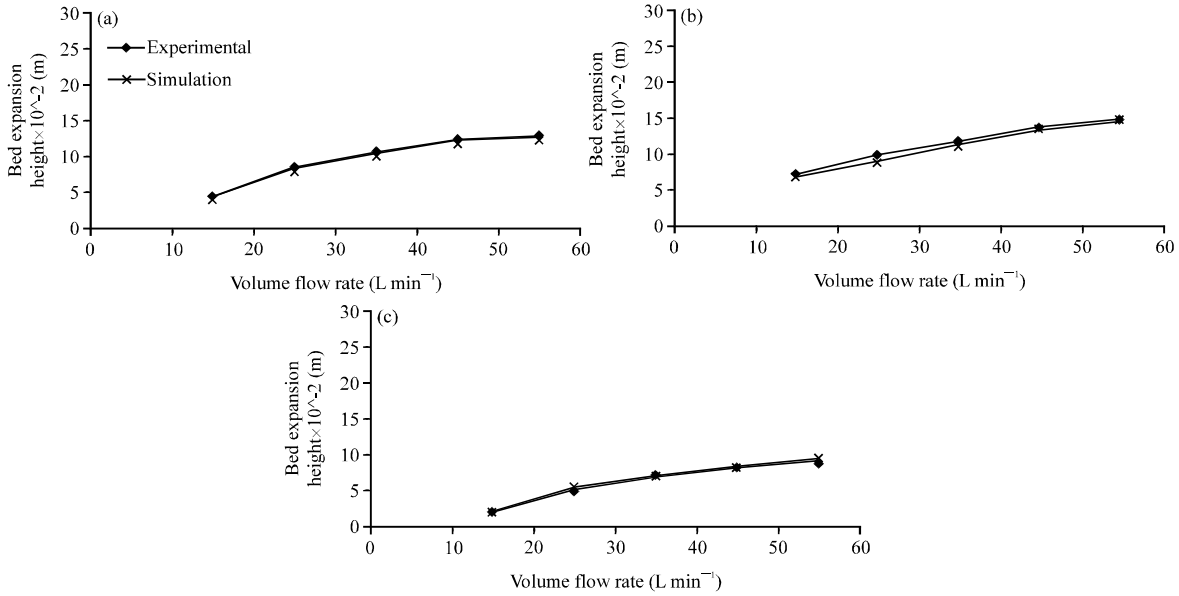

Fig. 10(a-c): Graph comparison between Fluent simulation and experimental, (a) 100 μm, (b) 500 μm and (c) 1000 μm

Table 5: Comparison between simulation and experiment on bed expansion height (CaO particle size: 100, 500 and 1000 μm, CaO-sand ratio: 50%)

	Expansion bed height×10^{-2} (m) at selected volume flow rate		
Volume flow rate (L min^{-1})	Experimental	Simulation	Difference (%)
100 μm CaO			
15	7.3	6.90	5.63
25	9.9	9.10	8.42
35	11.8	11.40	3.45
45	14.0	13.50	3.64
55	15.0	14.80	1.34
-	-	-	4.50
500 μm CaO			
15	4.5	4.20	6.90
25	8.5	8.20	3.59
35	10.8	10.20	5.71
45	12.5	12.10	3.25
55	13.0	12.50	3.92
-	-	-	4.68
1000 μm CaO			
15	2.0	2.10	4.88
25	5.0	5.40	7.69
35	7.0	6.70	4.38
45	8.0	8.30	3.68
55	9.0	9.50	5.41
-	-	-	5.21

CONCLUSION

Fluent software was successfully used to determine the capability of calcium oxide-sand fluidization contained in a CO_2 BFBAR. The 50% mixture used can perform fluidization perfectly without sticking out from the CO_2 BFBAR. The Eulerian multiphase model was applied and performed in a three dimensional numerical simulation. The height of the bed expansion was obtained for the particles size of 100, 500 and 1000 μm CaO-sand material with volumetric flow rates as a variables from 15 to 55 L min^{-1}. The comparison between computer simulation and experimental data in a cold model shows that the bed height expansion produced by computer simulation was almost similar to the one carried out in the experiments. The percentages of difference for three types of particle sizes used were small. The differences of 4.50, 4.68 and 5.21% fall within an acceptable range.

ACKNOWLEDGMENTS

The authors would like to express their appreciation to The Universiti Teknologi MARA (UiTM), Malaysia for giving the opportunity and supporting to do this biomass research study and also to the Universiti Sains Malaysia for The Research University Grant Scheme (Grant No. MEKANIK/811122) for providing financial support for this study.

REFERENCES

Anderson, J.D., 1995. Computational Fluid Dynamics: The Basics with Applications. McGraw-Hill Education, New York, USA., ISBN: 9780070016859, Pages: 547.

Azadi, M., 2011. Hydrodynamic modeling of the entrainment of Geldart a group particles in gas-solid fluidized bed: The effect of column diameter. Korean J. Chem. Eng., 28: 1599-1607.

Behjat, Y., S. Shahhosseini and S.H. Hashemabadi, 2008. CFD modeling of hydrodynamic and heat transfer in fluidized bed reactors. Int. Commun. Heat Mass Transfer, 35: 357-368.

Cooper, S. and C.J. Coronella, 2005. CFD simulations of particle mixing in a binary fluidized bed. Powder Technol., 151: 27-36.

Dogru, M., C.R. Howrath, G. Akay, B. Keskinler and A.A. Malik, 2002. Gasification of hazelnut shells in a downdraft gasifier. Energy, 27: 415-427.

FLUENT, 2009. FLUENT 6.3 User Guide. FLUENT Inc., Lebanon, NH., USA.

Gomez-Barea, A. and B. Leckner, 2010. Modeling of biomass gasification in fluidized bed. Prog. Energy Combust. Sci., 36: 444-509.

Ibrahim, W.Z.B.W., 2007. Towards a sustainable quarry industry in Malaysia. JURUTERA, December 2007, pp: 22-25.

Klass, D.L., 1998. Biomass for Renewable Energy, Fuels and Chemicals. Academic Press, San Diego, ISBN: 9780080528052, Pages: 651.

Lun, C.K.K., S.B. Sarage, D.J. Jeffrey and N. Cherpuny, 1984. Kinetic theories for granular flow: Inelastic particles in coquette flow and slightly inelastic particles in a general flow field. J. Fluid Mech., 140: 223-256.

Mahadzir, M.M., Z.A. Zainal, M. Iqbal and S.N. Soid, 2010. Characteristics on fluidization behaviors of 1000 ìm Cao-sand mixture by varying the percentage of CaO, air flow rate and pressure. J. Applied Sci., 10: 745-751.

Manovic, V., J.P. Charland, J. Blamey, P.S. Fennell, D.Y. Lu and E.J. Anthony, 2009. Influence of calcination conditions on carrying capacity of CaO-based sorbent in CO_2 looping cycles. Fuel, 88: 1893-1900.

McKendry, P., 2002. Energy production from biomass (part 2): Conversion technologies. Bioresour. Technol., 83: 47-54.

Midilli, A., M. Dogru, G. Akay and C.R. Howarth, 2002. Hydrogen production from sewage sludge via a fixed bed gasifier product gas. Int. J. Hydrogen Energy, 27: 1035-1041.

Munoz, M., F. Moreno, R.J. Morea, J. Ruiz and J. Arauzo, 2000. Low heating value gas on spark ignition engines. Biomass Bioenergy, 18: 431-439.

Nam, C.H., R. Pfeffer, R.N. Dave and S. Sundaresan, 2004. Aerated vibrofluidization of silica nanoparticles. Am. Inst. Chem. Eng. J., 50: 1776-1785.

Park, H.J., Y.K. Park and J.S. Kim, 2008. Influence of reaction conditions and the char separation system on the production of bio-oil from radiata pine sawdust by fast pyrolysis. Fuel Process. Technol., 89: 797-802.

Rezaiyan, J. and N.P. Cheremisinoff, 2005. Gasification Technologies: A Primer for Engineers and Scientists. CRC Press, USA., ISBN: 9780824722470, Pages: 360.

Singh, R.I., A. Brink and M. Hupa, 2013. CFD modeling to study fluidized bed combustion and gasification. Applied Therm. Eng., 52: 585-614.

Sridhar, G., P.J. Paul and H.S. Mukunda, 2001. Biomass derived producer gas as a reciprocating engine fuel: An experimental analysis. Biomass Bioenergy, 21: 61-72.

Syamlal, M., W. Rogers and J.S. O'Brien, 1993. MFIX documentation: Theory guide. Technical Note, DOE/METC-94/1004, NTIS/DE94000087. National Technical Information Service, Springfield, VA.

Van de Velden, M., J. Baeyens and I. Boukis, 2008. Modeling CFB biomass pyrolysis reactors. Biomass Bioenergy, 32: 128-139.

Vuthaluru, R., M. Tade, H. Vuthaluru, Y. Tsvetnenko, L. Evans and J. Milne, 2009. Application of CFD modelling to investigate fluidized limestone reactors for the remediation of acidic drainage waters. Chem. Eng. J., 149: 162-172.

Yang, W.C., 2003. Handbook of Fluidization and Fluid-Particle Systems. CRC Press, New York, ISBN: 9780824702595, Pages: 1868.

Zainal, Z.A., A. Rifau, G.A. Quadir and K.N. Seetharamu, 2002. Experimental investigation of a downdraft biomass gasifier. Biomass Bioenergy, 23: 283-289.

Zheng, J.L., 2008. Pyrolysis oil from fast pyrolysis of maize stalk. J. Anal. Applied Pyrolysis, 83: 205-212.